Hydrogen Transfer to Ketones Catalyzed by Shvo's Ruthenium Hydride Complex: A Mechanistic Insight

Aleix Comas-Vives, Gregori Ujaque,* and Agustí Lledós*

Unitat de Química Física, Departament de Química, Edifici Cn, Universitat Autònoma de Barcelona, 08193 Bellaterra, Catalonia, Spain

Received May 15, 2007

The Shvo catalyst is one of the most prominent examples of a hydrogen-transfer catalyst successfully applied in a broad scope of hydrogen-transfer processes. The reaction takes place by transferring a hydride (bonded to the metal center) and a proton (bonded to a ligand) to a double bond. The reaction mechanism for the hydrogen-transfer process, however, is a matter of controversy. Experimental studies by means of primary deuterium isotope effects on the hydrogenation of ketones via the active reducing form of the Shvo catalyst by the Casey and Bäckvall groups concluded that carbonyl hydrogenation is concerted. Nevertheless, it is not clear whether the reaction goes through an outer-sphere mechanism (without substrate coordination) or through an inner-sphere mechanism (with substrate coordination). In the present work several inner- and outer-sphere mechanisms are explored by means of theoretical methods. Energy reaction profiles clearly support the outer-sphere mechanism. Theoretically combined KIEs also suggests the concerted outer-sphere mechanism for this reaction. Some interesting features on the behavior of the Ru complex were found during the mechanistic investigations.

Introduction

The homogeneous hydrogenation of polar double bonds is one of the most useful reactions in organic synthesis.[1] Among the methodologies developed, hydrogen-transfer reactions have gained a prominent position in recent years.[2] They offer a viable alternative to the conventional hydrogenation using hydrogen gas due to its simplicity and the favorable properties of the reductant (generally alcohols) as environmentally friendly and also easy to handle.

The hydrogen transfer to ketones (or aldehydes) reactions are generally described by three general pathways. The "direct hydrogen transfer" is thought to work for main group elements, with no implication of a metal hydride intermediate. The "hydridic route", however, works for most transition metal catalysts, involving the participation of a metal hydride intermediate in the hydrogen-transfer process. The metal−ligand bifunctional catalysts, a concept developed to describe a type of hydrogenation catalysts where the metal has a hydridic hydrogen and a ligand an acidic hydrogen, operate through the hydridic route.[3] Recently, the so-called "ionic mechanism" has been also proposed for some transition-metal-catalyzed hydrogenations.[4]

Hydrogen transfer to ketones following the "hydridic route", and more specifically for catalysts that are monohydride complexes, has been suggested to go through two different pathways, "inner-sphere" and "outer-sphere" hydrogen-transfer mechanisms.[2b,c] In both mechanisms the hydride migrates to the carbonylic carbon atom. Nevertheless, whereas in the inner-sphere mechanism it is supposed that a metal alkoxide intermediate is formed (therefore, the substrate must become coordinated to the catalyst), in the outer-sphere mechanism the hydrogen transfer may proceed in a concerted manner (without the coordination of the substrate to the catalyst).

One of the most prominent examples of a hydrogen-transfer catalysts corresponds to the Shvo catalyst, $\{[Ph_4(\eta^5\text{-}C_4CO)]_2H\}\text{-}Ru_2(CO)_4H$ (**1**).[5] It has been applied successfully in a broad scope of hydrogen-transfer processes[5,6] such as hydrogenation of alkynes,[7] carbonyls,[8] and imines,[9] oxidation of alcohols[10] and amines,[11] and dynamic kinetic resolution of secondary alcohols[12] and primary amines[13] in combination with lipases. The Shvo

* Corresponding authors. E-mail: gregori@klingon.uab.es; agusti@klingon.uab.es.

(1) Clarke, M. L.; Roff, G. J. In *Handbook of Homogeneous Hydrogenation*; de Vries, J. G., Elsevier, C. J., Eds.; Wiley-VCH: Weinheim, 2007; Vol. 1, p 413.

(2) For reviews see: (a) Gladiali, S.; Alberico, E. *Chem. Soc. Rev.* **2006**, *35*, 226−236. (b) Samec, J. S. M.; Bäckvall, J.-E.; Andersson, P. G.; Brant, P. *Chem. Soc. Rev.* **2006**, *35*, 237−248. (c) Clapham, S. E.; Hadzovic, A.; Morris, R. H. *Coord. Chem. Rev.* **2004**, *248*, 2201−2237. (d) Bäckvall, J.-E. *J. Organomet. Chem.* **2002**, *652*, 105−111. (e) Noyori, R.; Hashiguchi, R. *Acc. Chem. Res.* **1997**, *30*, 97−102. (f) Zassinovich, G.; Mestroni, G.; Gladiali, S. *Chem. Rev.* **1992**, *92*, 1051−1069.

(3) (a) Noyori, R.; Ohkuma, T. *Angew. Chem.* **2001**, *113*, 40−75; *Angew. Chem., Int. Ed.* **2001**, *40*, 40−73. (b) Sandoval, C. A.; Ohkuma, T.; Muñiz, K.; Noyori, R. *J. Am. Chem. Soc.* **2003**, *125*, 13490−13503. (c) Fujii, A.; Hashiguchi, S.; Uematsu, N.; Ikariya, T.; Noyori, R. *J. Am. Chem. Soc.* **1996**, *118*, 2521−2522. (d) Uematsu, N.; Fujii, A.; Hashiguchi, S.; Ikariya, T.; Noyori, R. *J. Am. Chem. Soc.* **1996**, *118*, 4916−4917.

(4) (a) Bullock, R. M. *Chem.−Eur. J.* **2004**, *10*, 2366−2374. (b) Guan, H.; Iimura, M.; Magee, M. P.; Norton, J. R.; Zhu, G. *J. Am. Chem. Soc.* **2005**, *127*, 7805−7814.

(5) (a) Blum, Y.; Czarkie, D.; Rahamim, Y.; Shvo, Y. *Organometallics* **1985**, *4*, 1459−1461. (b) Shvo, Y.; Czarkie, D.; Rahamim, Y. *J. Am. Chem. Soc.* **1986**, *108*, 7400−7402.

(6) Karvembu, R.; Prabhakaran, R.; Natarajan, K. *Coord. Chem. Rev.* **2005**, *249*, 911−918.

(7) Shvo, Y.; Goldberg, I.; Czierkie, D.; Reshef, D.; Stein, Z. *Organometallics* **1997**, *16*, 133−138.

(8) Menashe, N.; Salant, E.; Shvo, Y. *J. Organomet. Chem.* **1996**, *514*, 97−102.

(9) Samec, J. S. M.; Bäckvall, J.-E. *Chem.−Eur. J.* **2002**, *8*, 2955−2961.

(10) Csjernyk, G.; Éll, A. H.; Fadini, L.; Pugin, B.; Bäckvall, J.-E. *J. Org. Chem.* **2002**, *67*, 1657−1662.

(11) (a) Samec, J. S. M.; Éll, A. H.; Bäckvall, J.-E. *Chem.−Eur. J.* **2005**, *11*, 2327−2334. (b) Éll, A. H.; Samec, J. S. M.; Brasse, C.; Bäckvall, J.-E. *Chem. Commun.* **2002**, 1144−1145.

(12) (a) Larsson, A. L. E.; Persson, B. A.; Bäckvall, J.-E. *Angew. Chem.* **1997**, *109*, 1256−1258; *Angew. Chem., Int. Ed.* **1997**, *36*, 1211−1212. (b) Persson, B. A.; Larsson, A. L. E.; Ray, M. L.; Bäckvall, J.-E. *J. Am. Chem. Soc.* **1999**, *121*, 1645−1650.

10.1021/om7004832 CCC: $37.00
Publication on Web 07/12/2007

Scheme 1. Equilibrium between Precursor and Active Species of the Shvo Catalyst

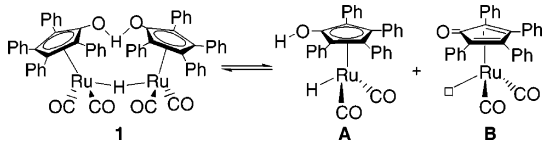

Scheme 2. Proposed Mechanisms for the Carbonyl Hydrogenation by Means of the Shvo Catalyst

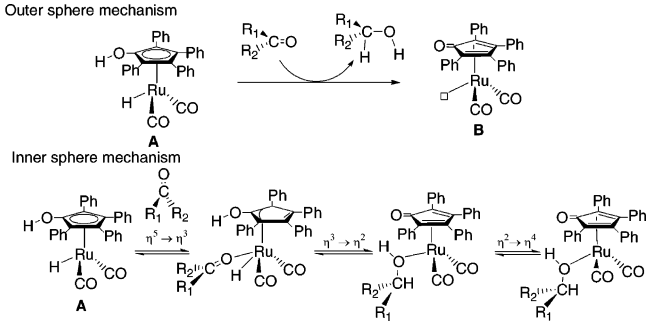

catalyst, synthesized two decades ago, is probably the first developed catalyst belonging to the so-called metal−ligand bifunctional catalysts. Since then, a number of metal−ligand bifunctional catalysts have been prepared based on Ru,[1,2,14] such as those by Noyori, Ru(diamine)(BINAP) and the Ru(η^6-arene)-TsDPEN,[3] and on other metal centers such as Rh, Ir, and Os.[15]

The Shvo catalyst under heating produces two active species, **A** and **B** (Scheme 1), which are able to hydrogenate unsaturated substrates or dehydrogenate saturated substrates, respectively. This equilibrium is what made the Shvo catalyst so versatile in hydrogen-transfer processes. In addition, the hydrogenation process starting from **A** generates **B**, and this one can be hydrogenated by alcohols or by H_2. In this last process, the explicit participation of a polar protic solvent molecule (EtOH) is playing a critical role in activating the hydrogen molecule.[16] This effect has also been reported in other systems.[3b,14b,17−19]

The reaction mechanism for the hydrogen-transfer process, however, is a matter of controversy. Studies by Casey by means of primary deuterium isotope effects on the hydrogenation of PhCHO via the active reducing form (**A**) of the Shvo tolyl analogue catalyst, [2,5-Ph_2-3,4-Tol_2(η^5-C_4COH)]Ru$(CO)_2$H, concluded that carbonyl hydrogenation is concerted without substrate coordination (outer-sphere mechanism, Scheme 2);[20] this conclusion was also supported by DFT calculations performed by the same authors.[21] Bäckvall, using a similar methodology, also reported a concerted mechanism for alcohol dehydrogenation using species **B**.[22] Nevertheless, although there is agreement in that catalytic reaction using the Shvo catalyst is concerted, Bäckvall suggested that the substrate coordinates the metal via a $\eta^5 \rightarrow \eta^3$ ring slippage[22,23] of the aromatic ligand, followed by a simultaneous β-hydride addition and a proton transfer to the unsatured organic substrate (inner-sphere mechanism, Scheme 2).

In imine hydrogenation there is also a similar mechanistic debate,[24−26] and although trapping experiments have provided additional information, they again have led to opposite conclusions concerning the mechanism.[21,26] In ketone hydrogenation this approach is not possible because of the high lability of alcohol complexes.[27] In related systems such as the Ru(η^6-arene)TsDPEN and the Ru(η^6-arene)(amino alcohol) catalysts, Noyori, Casey, and Andersson have provided evidence, both experimentally and theoretically, that carbonyl hydrogenation takes place by an outer-sphere mechanism via a six-membered transition state.[28]

In the present work we performed an extensive theoretical analysis on both the inner- and outer-sphere mechanisms, trying to clarify the mechanism of this useful reaction. For the inner-sphere mechanism, in addition to the concerted pathway two additional pathways involving the substrate coordination were also evaluated. For the outer-sphere mechanism, a concerted reaction without substrate coordination was examined in detail.

Computational Details

An extensive mechanistic analysis was performed on a model reaction system. Formaldehyde was selected as a substrate, whereas the Shvo catalyst was modeled by [(η^5-C_4H_4COH)Ru$(CO)_2$H]; the phenyl substituents of the aromatic ligand, hereafter named CpOH, were replaced by hydrogens. These four H's were calculated using the 6-31G basis set, and the other main group elements (C, O, the rest of H) were calculated using the 6-31G(d,p) basis set. The effective core potential LANL2DZ[29] along with its associated basis set was employed for Ru.

Calculations for the model system were carried out using the program package Gaussian03[30] at density functional theory (DFT) level by means of the hybrid B3LYP functional.[31] All the calculations were done without any geometrical constraints. Ad-

(13) Paetzold, J.; Bäckvall, J.-E. *J. Am. Chem. Soc.* **2005**, *127*, 17620−17621.

(14) (a) Gómez, M.; Jansat, S.; Muller, G.; Aullón, G.; Maestro, M. A. *Eur. J. Inorg. Chem.* **2005**, 4341−4351. (b) Ito, M.; Hirakawa, M.; Murata, K.; Ikariya, T. *Organometallics* **2001**, *20*, 379−381. (c) Abdur-Rashid, K.; Clapham, S. E.; Hadzovic, A.; Harvey, J. N.; Lough, A. J.; Morris, R. H. *J. Am. Chem. Soc.* **2002**, *124*, 15104−15118.

(15) (a) Wu, X.; Vinci, D.; Ikariya, T.; Xiao, J. *Chem. Commun.* **2005**, 4447−4449. (b) Clapham, S. E.; Morris, R. H. *Organometallics*, **2005**, *24*, 479−481. (c) Mao, J.; Baker, D. C. *Org. Lett.* **1999**, *1*, 841−843. (d) Martin, M.; Sola, E.; Tejero, S.; Andres, J. L.; Oro, L. A *Chem.−Eur. J.* **2006**, *12*, 4043−4056.

(16) Casey, C. P.; Johnson, J. B.; Singer, S. W.; Cui, Q. *J. Am. Chem. Soc.* **2005**, *127*, 3100−3109.

(17) Rautenstrauch, V.; Hoang-Cong, X.; Churlaud, R.; Abdur-Rashid, K.; Morris, R. H. *Chem.−Eur. J.* **2003**, *9*, 4954−4967.

(18) Hedberg, C.; Källström, K.; Arvidsson, P. I.; Brandt, P.; Andersson, P. G. *J. Am. Chem. Soc.* **2005**, *127*, 15083−15090.

(19) Comas-Vives, A.; González-Arellano, C.; Corma, A.; Iglesias, M.; Sánchez, F.; Ujaque, G. *J. Am. Chem. Soc.* **2006**, *128*, 4756−4765.

(20) Casey, C. P.; Singer, S.W.; Powell, D. R.; Hayashi, R. K.; Kavana, M. *J. Am. Chem. Soc.* **2001**, *123*, 1090−1100.

(21) Casey, C. P.; Bikzhanova, G. A.; Cui, Q.; Guzei, I. A. *J. Am. Chem. Soc.* **2005**, *127*, 14062−14071 (see also Supporting Information therein).

(22) Johnson, J. B.; Bäckvall, J.-E. *J. Org. Chem.* **2003**, *68*, 7681−7684.

(23) (a) Csjernyik, G.; Éll, A. H.; Fadini, L.; Pugin, B.; Bäckvall, J.-E. *J. Org. Chem.* **2002**, *67*, 1657−1662. (b) In ref 7 Shvo proposed the same ring slippage for alkyne hydrogenation.

(24) (a) Casey, C. P.; Bikzhanova, G. A.; Guzei, I. A. *J. Am. Chem. Soc.* **2006**, *128*, 2286−2293. (b) Casey, C. P.; Johnson, J. B. *J. Am. Chem. Soc.* **2005**, *127*, 1883−1894.

(25) (a) Samec, J. S. M.; Éll, A. H.; Bäckvall, J.-E. *Chem. Commun.* **2004**, 2748−2749. (b) Éll, A. H.; Johnson, J. B.; Bäckvall, J.-E. *Chem. Commun.* **2003**, 1652−1653.

(26) Samec, J. S. M.; Éll, A. H.; Åberg, J. B.; Privalov, T.; Eriksson, L.; Bäckvall, J.-E. *J. Am. Chem. Soc.* **2006**, *128*, 14293−14305.

(27) Casey, C. P.; Bikzhanova, G. A.; Bäckvall, J.-E.; Johansson, L.; Park, J.; Kim, Y. H. *Organometallics* **2002**, *21*, 1955−1959.

(28) (a) Yamakawa, M.; Ito, H.; Noyori, R. *J. Am. Chem. Soc.* **2000**, *122*, 1466−1478. (b) Casey, C. P.; Johnson, J. B. *J. Org. Chem.* **2003**, *68*, 1998−2001. (c) Alonso, D. A.; Brandt, P.; Nordin, S. J. M.; Andersson, P. G. *J. Am. Chem. Soc.* **1999**, *121*, 9580−9588.

(29) Hay, P. J.; Wadt, W. R. *J. Chem. Phys.* **1985**, *82*, 270−283.

(30) Frisch, M. J.; et al. *Gaussian03*; Gaussian, Inc.: Wallingford, CT, 2004.

(31) (a) Becke, A. D. *J. Chem. Phys.* **1993**, *98*, 5648−5652. (b) Lee, C.; Yang, W.; Parr, R. G. *Phys. Rev. B* **1988**, *37*, 785−789. (c) Stephens, P. J.; Devlin, F. J.; Chabalowski, C. F.; Frisch, M. J. *J. Phys. Chem.* **1994**, *98*, 11623−11627.

ditional MP2[32] and CCSD(T)[33] single-point energy calculations were also performed (see Supporting Information).

The most energetically favorable inner- and outer-sphere mechanisms were evaluated using a complete Shvo catalyst (including the [$Ph_4(\eta^5$-$C_4COH)$] ligand) by means of the Jaguar program suite.[34] The 6-31G(d,p) basis set was used for all the atoms except for Ru. For the latter, the Los Alamos relativistic ECP was used, together with a Jaguar-developed triple-ζ modification of the standard Los Alamos basis set to describe the outermost core and valence 4s, 4p, 4d, and 5s electrons (LACV3P basis).

For the saddle points the existence of only one imaginary frequency was checked by means of analytical frequency calculations. Polarization functions were added to hydrogens of the phenyl rings: 6-31G(d,p). Solvent effects (THF) were included using the CPCM[35] model performing single-point calculations on gas-phase optimized geometries. KIEs were also evaluated as shown in eqs 1 and 2 using the calculated free energies at 298.15 K. The concerted pathway for the complete system was optimized with Gaussian, along with the frequency analysis.

$$\Delta G_X = G_{TS} - G_R \qquad X = H, D \tag{1}$$

$$KIE = k_H/k_D = \exp[(\Delta G_D - \Delta G_H)/RT] \tag{2}$$

Results and Discussion

This section is divided in two subsections. In the first one, three different inner-sphere mechanisms are discussed. Two of them start with an initial coordination of the substrate (formaldehyde) to the catalyst, whereas in the last one the coordination is simultaneous to the hydrogen transfer. In the second subsection a concerted pathway for the outer-sphere mechanism is discussed.

Inner-Sphere Mechanisms. In this section three inner-sphere mechanisms are analyzed. Two of them involve the replacement of one of the occupied coordination sites of the metal center by the substrate. The first one involves the replacement of one CO, whereas the second one consists on the ring slippage of the aromatic ring to accommodate the substrate. In the third one, the incorporation of the substrate to the coordination sphere is simultaneous to the hydrogen transfer.

Substrate Coordination by Replacing the CO Ligand. The initial reactants and final products shown in Figure 1 are the same for all the studied mechanisms. Two rotamers have been localized for the active reducing species of the Shvo catalyst, **a1** and **a2**. These two conformers differ energetically only by 0.2 kcal/mol, indicating that the different rotamers are equally accessible. Once the hydrogenation occurs, the dehydrogenated form of the catalyst (**b**) and the hydrogenated product, methanol, are produced. Reactants and products are isoenergetic in the gas phase, and when solvent effects are taken into account, the reaction energy is −3.5 kcal/mol.

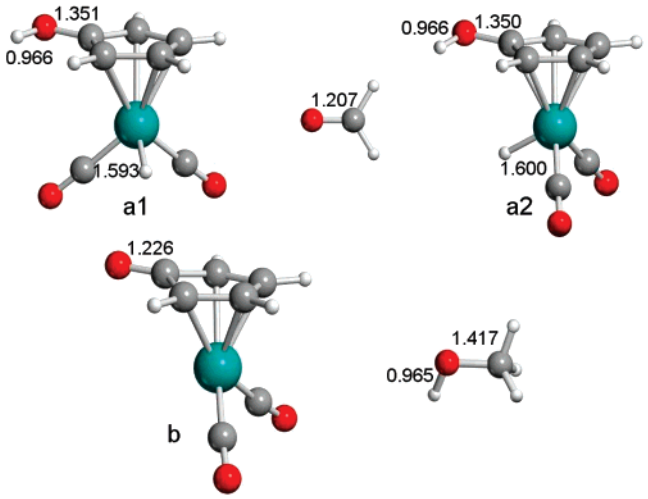

Figure 1. Optimized structures for the initial reactants and final products of the hydrogenation reaction. Distances in Å.

Scheme 3. Reaction Steps of the CO Leaving Mechanism

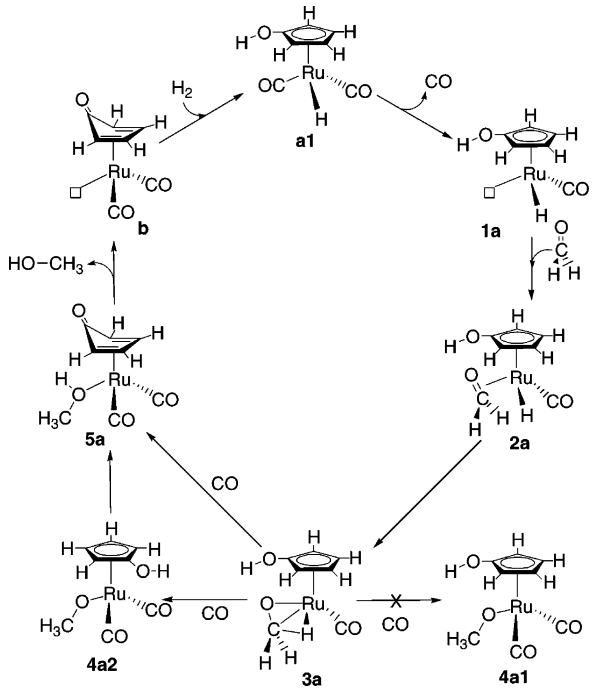

In the Scheme 3 are shown the steps found for this mechanism. It is initiated with the generation of a vacant site by a CO bond-breaking process and the subsequent coordination of formaldehyde.[36] After that, a hydride transfer to the carbonylic carbon takes place followed by the proton transfer to the carbonylic oxygen atom, giving raise to the final product, methanol.

The CO departure step was found to be endothermic by 51.2 kcal/mol (**1a**). This highly endothermic process is in agreement with experimental results where Casey and co-workers found that the exchange of a CO by a ^{13}CO molecule was very slow

(32) (a) Møller, C.; Plesset, M. S. *Phys. Rev.* **1934**, *46*, 618−622. (b) Head-Gordon, M.; Pople, J. A.; Frisch, M. J. *Chem. Phys. Lett.* **1988**, *153*, 503−506. (c) Frisch, M. J.; Head-Gordon, M.; Pople, J. A. *Chem. Phys. Lett.* **1990**, *166*, 275−280. (d) Frisch, M. J.; Head-Gordon, M.; Pople, J. A. *Chem. Phys. Lett.* **1990**, *166*, 281−289. (e) Head-Gordon, M.; Head-Gordon, T. *Chem. Phys. Lett.* **1994**, *220*, 122−128. (f) Sæbø, S.; Almlöf, J. *Chem. Phys. Lett.* **1989**, *154*, 83−89.

(33) (a) Čizek, J. *Adv. Chem. Phys.* **1969**, *14*, 35−89. (b) Purvis G. D., III; Bartlett, R. J. *J. Chem. Phys.* **1982**, *76*, 1910−1918. (c) Scuseria, G. E.; Janssen, C. L.; Schaefer, H. F., III. *J. Chem. Phys.* **1988**, *89*, 7382−7387. (d) Scuseria, G. E.; Schaefer, H. F., III. *J. Chem. Phys.* **1989**, *90*, 3700−3703. (e) Pople, J. A.; Head-Gordon, M.; Raghavachari, K. *J. Chem. Phys.* **1987**, *87*, 5968−5975.

(34) *Jaguar 5.5*; Schrödinger, L.L.C.: Portland, OR, 1991−2003.

(35) (a) Barone, V.; Cossi, M. *J. Phys. Chem. A* **1998**, *102*, 1995−2001. (b) Cossi, M.; Rega, N.; Scalmani, G.; Barone, V. *J. Comput. Chem.* **2003**, *24*, 669−681.

(36) For aldehyde or ketone coordination, either η^1 or η^2, see for instance: (a) Bergamo, M.; Beringhelli, T.; D'Alfonso, G.; Maggioni, D.; Mercandelli, P.; Sironi, A. *Inorg. Chim. Acta* **2003**, *350*, 475−485. (b) Méndez, N. Q.; Arif, A. M.; Gladysz, J. A. *Angew. Chem., Int. Ed.* **1990**, *29*, 1473−1474. (c) Méndez, N. Q.; Mayne, C. L.; Gladysz, J. A. *Angew. Chem., Int. Ed.* **1990**, *29*, 1475−1476. (d) Méndez, N. Q.; Seyler, J. W.; Gladysz, J. A. *J. Am. Chem. Soc.* **1993**, *115*, 2323−2334. (e) Boone, B. J.; Klein, D. P.; Seyler, J. W.; Méndez, N. Q.; Arif, A. M.; Gladysz, J. A. *J. Am. Chem. Soc.* **1996**, *118*, 2411−2421.

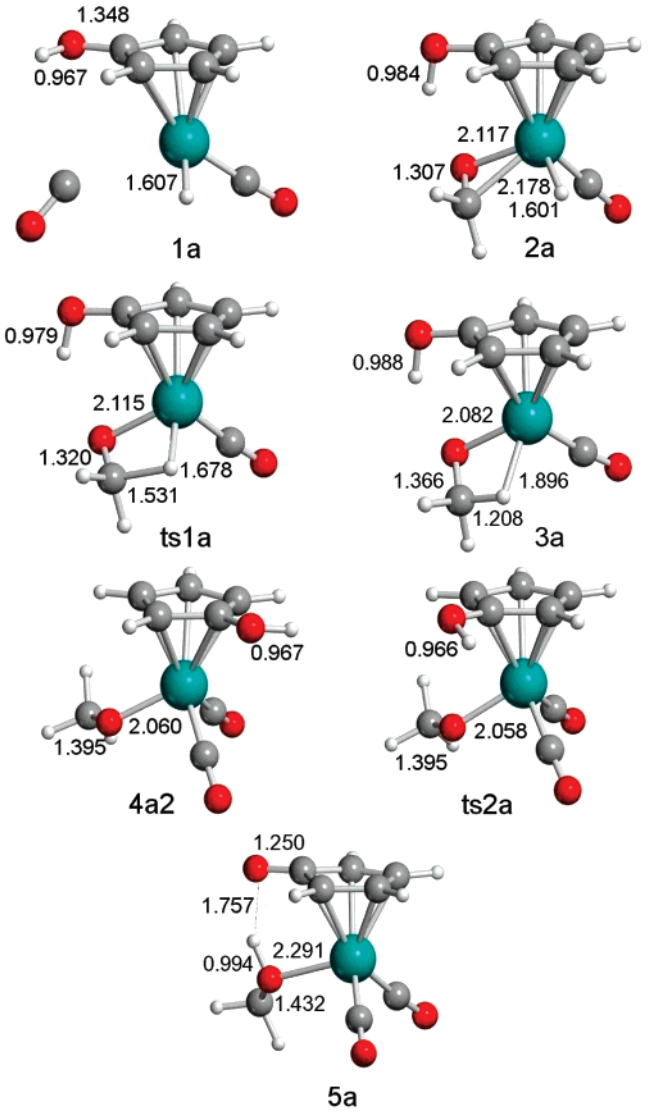

Figure 2. Located stationary points for the CO leaving mechanism. Distances in Å.

unless the reaction took place under fluorescent light.[20] Although this process should be entropically favored, the calculated free energy difference is still too large: 38.7 kcal/mol.

The CO leaving generates a vacant site that can be occupied by the substrate, forming intermediate **2a**. In this intermediate the formaldehyde is η^2-coordinated with Ru−C and Ru−O distances of 2.178 and 2.117 Å, respectively. The energy of this intermediate, **2a**, is 23.8 kcal/mol with respect to the initial reactants. Figure 2 shows the intermediates and transition states involved in this reaction mechanism.

Once the formaldehyde is coordinated to the catalyst, the hydrogen-transfer process may proceed following two sequences: the initial transfer of the CpOH proton to the carbonylic oxygen atom or the initial hydride transfer to the carbonylic carbon atom. The hydride transfer to the carbonylic carbon has a barrier of 7.9 kcal/mol, giving rise to intermediate **3a**. The transition state for this step, **ts1a**, is characterized by a forming C−H bond distance of 1.531 Å, whereas the Ru−H breaking distance is 1.678 Å. This step is endothermic by 5.7 kcal/mol, with the product **3a** having an agostic interaction with the metal via the newly formed C−H bond. The C−H bond distance is 1.208 Å, whereas the Ru···H distance is 1.896 Å. As far as the C═O distance is concerned, it is elongated from 1.307 Å to 1.320 Å and to 1.366 Å in the reactant, **2a**, transition state, **ts1a**, and product, **3a**, respectively.

The coordination site occupied by the agostic interaction can be subsequently replaced by a CO molecule. Depending on the relative position of the CpOH ligand, the proton-transfer step can be barrierless or show a very low barrier. When the position of the proton is near the alkoxide ligand, an intermediate (**4a1** in Scheme 3) could not be located because the proton transfer takes place spontaneously. An alkoxide intermediate, **4a2**, could be located only when the proton of the CpOH ring was in the opposite site of the alkoxide ligand. The energy barrier for the proton transfer from intermediate **4a2** is 3.3 kcal/mol, mainly corresponding to the CpOH ring rotation. This step is exothermic by 19.7 kcal/mol, and the final product, methanol, remains bonded to the catalyst through an agostic interaction. The energy profile for this reaction is presented in Figure 3.

We also evaluated a pathway that once the formaldehyde is coordinated, intermediate **2a**, the mechanism goes through the inverse hydrogen-transfer order, starting with the proton transfer followed by the migration of the hydride. Results are quite similar to the previous mechanism with the opposite transfer order (vide supra). The proton and hydride migrations barriers are 9.7 and 10.5 kcal/mol, respectively, slightly higher than those found in the preceding mechanism.

The inclusion of solvent effects (THF) by means of the CPCM method does not significantly change the energy profile. The CO leaving step is the most affected one, by decreasing the energy 5.5 kcal/mol; the overall reaction becomes slightly exothermic by 3.5 kcal/mol (Figure 3). Thus, the high reported endothermicity for the CO leaving process brought us to reject this mechanism as a feasible mechanism for this process, in agreement with the experimental results.[20]

Substrate Coordination with CpOH Ring Slippage. A different pathway to coordinate the unsaturated substrate to the Ru center involves a ring slippage. This process creates a vacant site that can be occupied by the formaldehyde. In Scheme 4 is presented the general pathway found for this mechanism.

The initial structure found for this reaction mechanism presents a hydrogen bond between the formaldehyde and the acidic hydrogen of the CpOH ligand; the O···H distance is 1.793 Å (see Figure 4). The next step should correspond to the coordination of the formaldehyde to the catalyst. The transition state for this step, **ts1b**, shows that the substrate coordination and the ring slippage take place simultaneously. The Ru−O distance in **ts1b** is 2.502 Å. The ring slippage is observed by the Ru−C distances: two carbon atoms of the CpOH ring remain close to the metal with Ru−C bond distances of 2.311 and 2.358 Å, respectively, whereas the other Ru−C distances are elongated to 2.823, 3.154, and 2.886 Å, respectively. These distances in transition state **ts1b** indicate that the CpOH ring becomes η^2-coordinated to the metal center. Two additional transition states are expected to be formed by simple rotation of the CpOH ligand. Their geometries and energies, however, are expected to be very similar. We calculated the isomers of the formed intermediate **2b**; if the OH group is on the symmetrical position of **2b** (with the OH at one bond distance of the coordinated double bond), forming the **2b2** intermediate, the energy is very similar, 16.3 kcal/mol. Nevertheless, we did not find the isomer where the OH group is on the opposite side of the coordinated double bond; the geometry optimizations led to losing the ketone, generating the η^5-CpOH ring coordination.

In the formed intermediate, **2b**, the Ru−O bond distance is 2.206 Å. The ring coordination in **2b** can also be described by a η^2-coordination mode (as in the transition state). The Ru−C

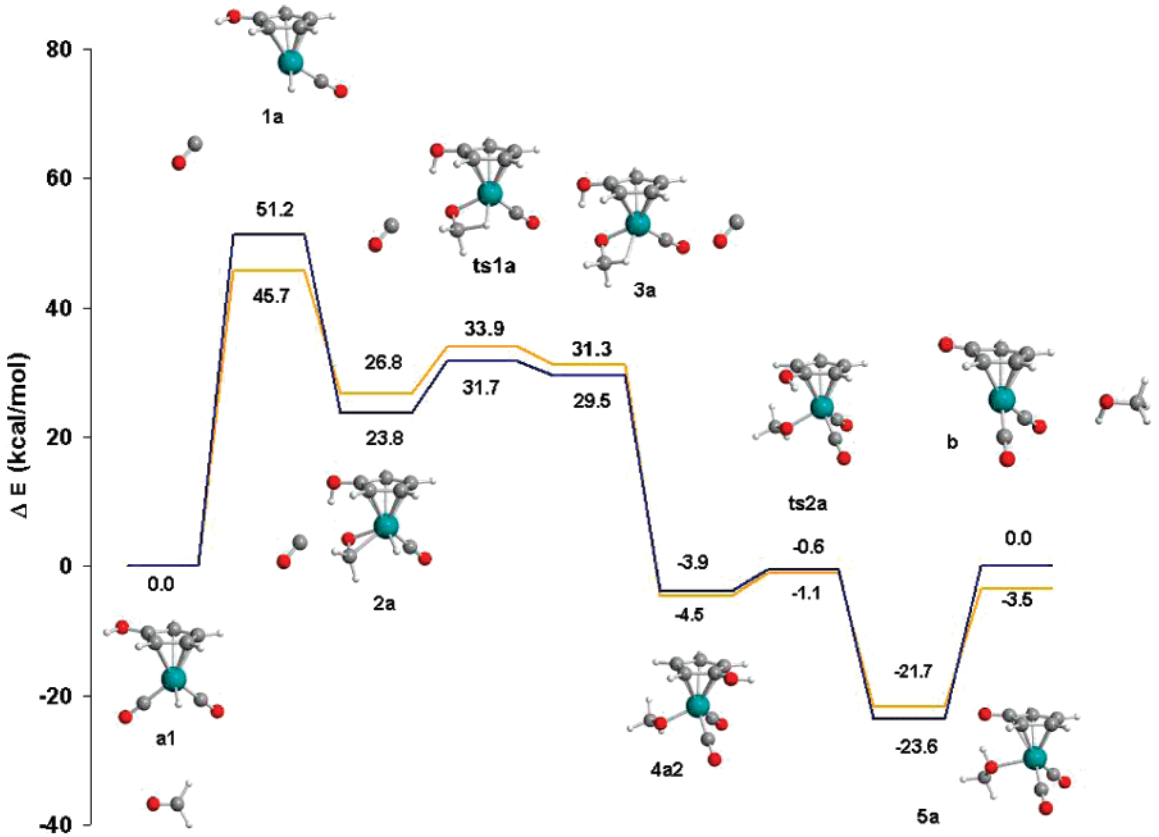

Figure 3. Energy profile for the CO leaving mechanism at the B3LYP level in the gas phase (blue) and solution (orange).

Scheme 4. Reaction Steps of the Stepwise $\eta^5 \rightarrow \eta^2$ Ring Slippage Mechanism

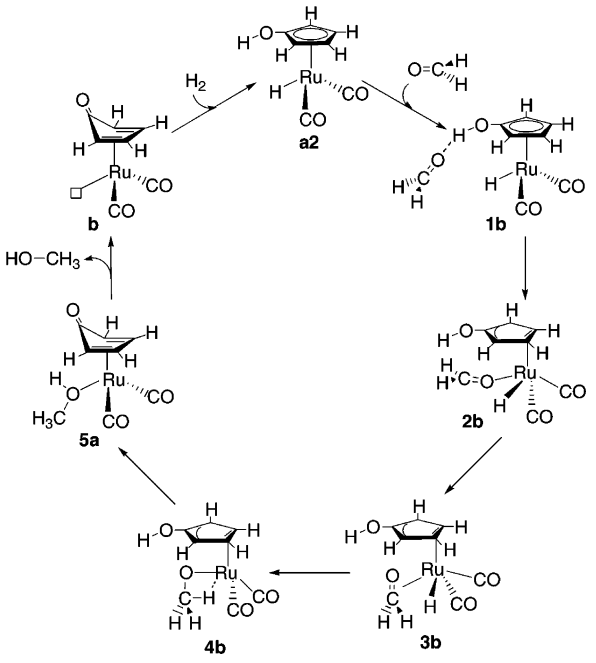

distances for the coordinating carbon atoms are 2.312 and 2.479 Å. For the noncoordinated carbons the Ru−C distances are 3.103, 3.559, and 3.216 Å, respectively. The addition of formaldehyde to the complex shortens the metal−ligand distances. Thus, the Ru−H distance is 1.575 Å in **2b** and 1.606 Å in **1b**; thus, the Ru−H distance has been considerably affected by the change in the geometry from structure **1b** to **2b**.

Both the transition state, **ts1b**, and the intermediate, **2b**, present a η^2-coordination mode of the aromatic ring. These results are different from those initially proposed where the ring slippage was changing the coordination mode from η^5 to η^3. Nevertheless, recent theoretical studies on the ring slippage of the Cp ring by the addition of a new ligand on related transition metal complexes showed that the most stable coordination mode of the Cp is η^2 once the ligand is coordinated[37] and also in some transition states of the ligand coordination step.[38]

The next step in the catalytic cycle corresponds to the change of the coordination mode of the substrate from η^1 to η^2 coordination going from intermediates **2b** to **3b**. Furthermore, the carbonylic carbon atom should be oriented toward the hydride in order to allow the hydride migration. The step involving these two changes is thermodynamically endothermic by 4.2 kcal/mol. Intermediate **3b** has Ru−O and Ru−C distances of 2.296 and 2.424 Å, respectively. At this point the hydrogen-transfer process starts by a pathway quite similar to that described in the previous section. The carbonyl group is inserted into the Ru−H bond, giving rise to intermediate **4b**. The transition state, **ts2b**, is located only 1.5 kcal/mol above the intermediate **3b**. This step is exothermic by 4.4 kcal/mol. The **ts2b** structure is characterized by a C−H bond forming distance of 1.689 Å. The atoms involved in the insertion have a Ru−O−C−H torsion angle of −14.1°. The C═O distance of the formaldehyde is gradually enlarged from 1.253 Å in **3b**, to 1.276 Å in **ts2b**, and to 1.371 Å in **4b**, therefore becoming a single C−O bond. As far as the intermediate **4b** is concerned, it contains an agostic interaction between the recently formed C−H bond and the Ru atom, as shown by the large C−H distance, 1.169 Å. The Ru−O distance of the alkoxide ligand

(37) Veiros, L. F. *Organometallics* **2000**, *19*, 5549−5558.
(38) Fan, H.-J.; Hall, M. B. *Organometallics* **2001**, *20*, 5724−5730.

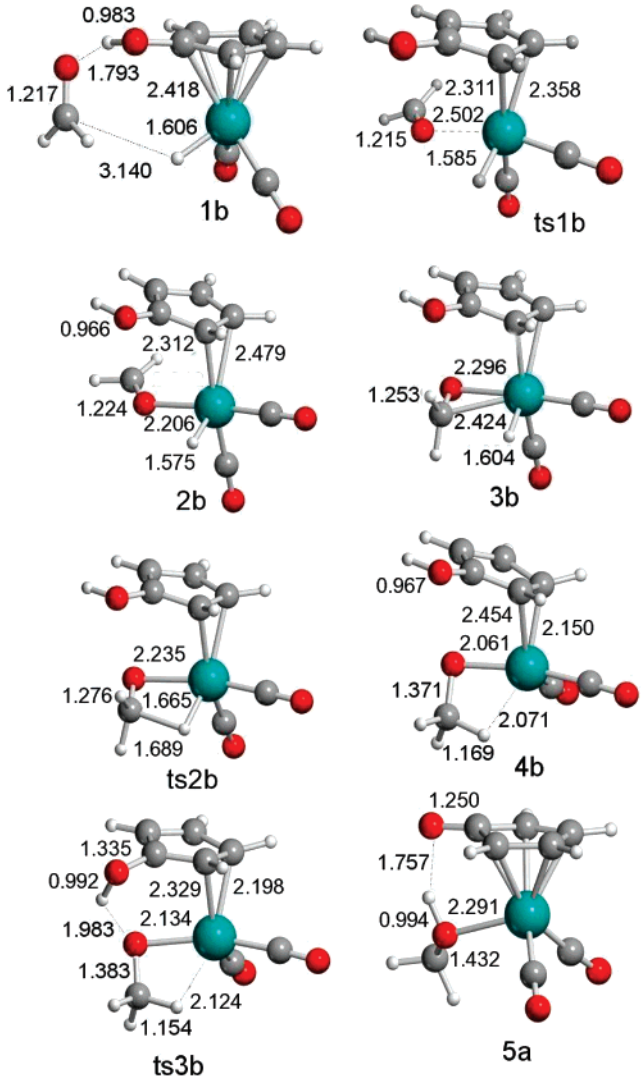

Figure 4. Located stationary points for the stepwise $\eta^5 \rightarrow \eta^2$ ring slippage mechanism. Distances in Å.

is 2.061 Å, being shortened almost 0.3 Å with respect to intermediate **3b**.

The last step, the proton transfer to the alkoxy oxygen, gives rise to the final product, ethanol. This step is exothermic by 41.6 kcal/mol. The corresponding transition state, **ts3b**, has a relatively low energy barrier, 4.2 kcal/mol. Although the proton transfer does not involve the CpOH ring rotation, the **ts3b** structure is also unique. The O−H bond-breaking distance is not very enlarged, 0.992 Å, compared to that in intermediate **4b**, 0.967 Å; the length of the newly forming O−H bond is 1.983 Å. The change in the C−C−O−H dihedral angle on going from intermediate **4b** to **ts3b** is quite large (from −1.8° to −111.5°), indicating that the OH group from the CpOH ligand must be located in the proper alignment for the proton transfer to take place.

The energy profile for this mechanism is presented in Figure 5. The highest relative energy barrier concerns the simultaneous aldehyde coordination with the $\eta^5 \rightarrow \eta^2$ ring slippage. Nevertheless, the highest point within the energy profile is the **ts2b** structure, where the hydride migration is taking place. The energy difference between the lowest energy intermediate and the highest energy transition state is 34.3 kcal/mol. Other possibilities could be considered from structure **4b** to reach final products, because the hydride migration leaves a vacant site that could be occupied by the ring changing its hapticity. In any case, this mechanism must go through **ts2b**, and therefore, the energy barrier to overcome is higher than 30 kcal/mol.

Concerning the calculations in solution, there are no significant changes. The major differences are for **1b** and products (**b** + CH_3OH) with energy changes of 3.3 and 3.5 kcal/mol, repectively. The energy difference between the minima **1b** and the transition state **ts2b** including solvent effects is 33.0 kcal/mol. These results indicate that the stepwise $\eta^5 \rightarrow \eta^2$ mechanism is more favorable than the stepwise mechanism involving the CO leaving, 45.7 versus 33.0 kcal/mol (in solution), although the energy barrier is still too high.

Concerted Pathway with Simultaneous Substrate Coordination and Ring Slippage. The third inner-sphere mechanism analyzed corresponds to the concerted hydrogen transfer having the substrate in the coordination sphere of the catalyst. Figure 6 shows the structures of the species involved in this reaction pathway.

The initial structure corresponds to an intermediate with the formaldehyde hydrogen bonded to the catalyst, **1b**, the same structure presented in the previous section. The concerted hydrogen transfer produces intermediate **2c**, where the ethanol product is weakly coordinated to the metal center through an agostic interaction. The Ru−H distance is 1.959 Å, whereas the newly formed C−H bond distance is 1.155 Å, clearly showing the agostic interaction. During this process, the CpOH ligand loses a proton, breaking the ring aromaticity, becoming bonded to the Ru by a η^4-coordination. The dihedral angle of the four coordinated carbon atoms is −0.2°; the dihedral angles of the carbonylic carbon atom within the ring are 8.3° and −7.9°, showing that this carbon atom is actually out of the plane of the four coordinated atoms.

The Ru−C distances for the four coordinated carbon atoms are 2.288, 2.224, 2.223, and 2.282 Å, respectively. The Ru−C distance for the carbon atom that is out of the plane in **2c** is 2.508 Å. In this step there is also a change of the nature of the C−O bond of the ring, changing from a single bond (1.338 Å) to a double bond (1.241 Å). The hydrogen bond distance between the OH of the formed methanol and the oxygen atom from the formed ketone is 1.773 Å.

In the transition state for this step, **ts1c**, the newly forming C−H and O−H bonds follow a different trend. The C−H forming bond is quite advanced with a distance of 1.233 Å, whereas the O−H forming bond distance is 1.884 Å, indicating a rather small interaction; the O−H bond distance of the CpOH ring is practically unchanged, going from 0.983 Å in **1b** to 0.988 Å in **ts1c**. In order to corroborate that **ts1c** actually connects the **1b** and **2c** intermediates, we performed an IRC calculation.[39] Starting from structure **ts1c** we obtained **1b** and **2c**, the initial reactant and the final product, respectively, and no other intermediates were found on this pathway.

Concerning the CpOH ligand in the **ts1c**, it is η^3-coordinated to the Ru atom. The Ru−C distances for the coordinated carbons atoms are 2.372, 2.296, and 2.463 Å, whereas the Ru−C distances for the other carbon atoms are 2.767 and 2.868 Å, respectively. It is remarkable that η^3 coordination was observed only in structure **ts1c**. This hapticity has already been observed in other transition metal complexes during a ligand substitution process.[38] In fact, the $\eta^5 \rightarrow \eta^3$ ring slippage allows the η^2 coordination of the unsaturated substrate to the metal; the Ru−O and Ru−C distances are 2.300 and 2.475 Å, respectively. The

(39) (a) Fukui, K. *Acc. Chem. Res.* **1981**, *14*, 363−368. (b) Gonzalez, C.; Schlegel, H. B. *J. Chem. Phys.* **1989**, *90*, 2154−2161. (c) Gonzalez, C.; Schlegel, H. B. *J. Phys. Chem.* **1990**, *94*, 5523−5527.

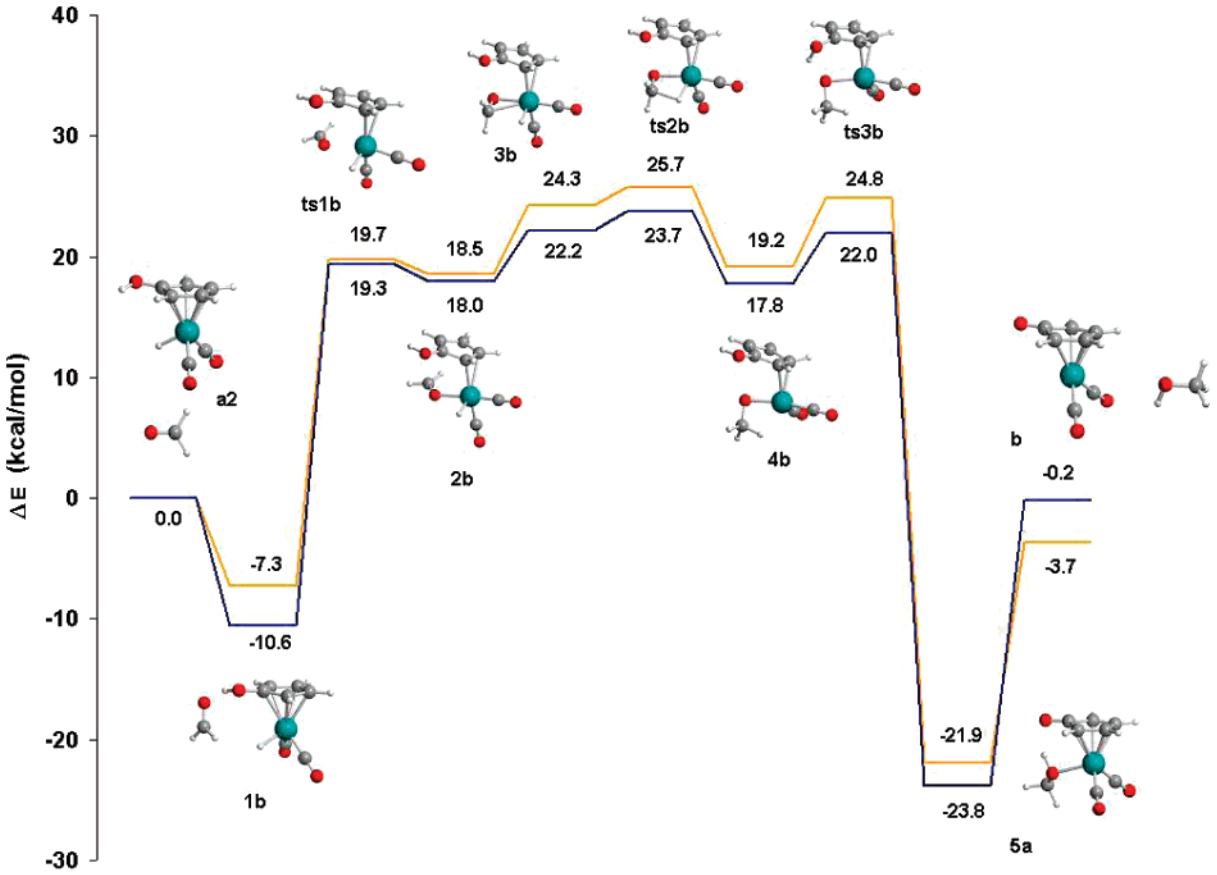

Figure 5. Energy profile for the stepwise $\eta^5 \rightarrow \eta^2$ ring slippage mechanism at the B3LYP level in the gas phase (blue) and in solution (orange).

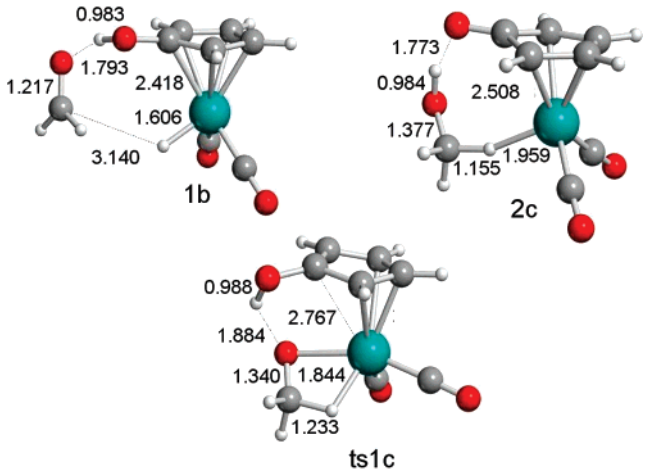

Figure 6. Optimized structures of the transition state **ts1c** and minima structures that connect **1b** and **2c**. Distances in Å.

C═O bond distance of the formaldehyde is 1.340 Å, so it has been enlarged by 0.123 Å in the transition state compared to the reactant **1b**, where the distance is 1.217 Å.

The barrier height for this pathway is 36.0 kcal/mol, with an associated reaction energy of −2.3 kcal/mol. The solvent effects do not significantly modify the energetics of the reaction: the energy barrier is 34.6 kcal/mol, whereas the reaction energy is −4.5 kcal/mol.

Outer-Sphere Mechanism. Concerted Hydrogen-Transfer Mechanism. In this mechanism, the hydrogen transfer takes place without coordination of the substrate on the catalyst. The proton and hydride transfers occur simultaneously in a single step. The initial intermediate **1b** and the final product **2c** are the same as those obtained in the previous concerted pathway. Nevertheless, the major difference between these two pathways relies on the nature of the transition state.

In the transition state for this step, **ts1d**, the newly forming C−H and O−H bond distances are 1.432 and 1.325 Å, respectively (Figure 7). The C−O distance for the substrate is 1.278 Å, slightly shorter than in structure **ts1c** (1.340 Å). Surprisingly, this transition state links exactly the same intermediates, **1b** and **2c**, as that found in the concerted $\eta^5 \rightarrow \eta^3$ ring slippage pathway, respectively. As far as the energies are concerned, the relative energy barrier found in this process is 9.1 kcal/mol in the gas phase and 7.7 kcal/mol in solution, in good agreement with experiment and previous computational work.[21] Casey and co-workers reported a value of $\Delta H^{\ddagger} = 12.0 \pm 1.5$ kcal/mol for the reduction of PhCHO in THF-d_8 with 0.1 mol/L of H_2O or D_2O using the Shvo tolyl analogue.[20] More recently, they reported the barrier for the analogous process in dry THF-d_8; $\Delta H^{\ddagger} = 11.2 \pm 0.9$ kcal/mol.[40] In their computational study of the concerted mechanism Casey, Cui, and co-workers reported a barrier height of 13.8 kcal/mol, in agreement with the results presented here. Figure 8 shows the energy profile for both concerted pathways in solution and gas phase.

After the analysis of several inner- and outer-sphere mechanisms on a model system, computational results strongly support the outer-sphere mechanism with no coordination of the substrate in the catalyst. The reported barrier of 9.1 kcal/mol in the gas phase (7.7 kcal/mol in solution) is in agreement with previously determined experimental energy barriers; $\Delta H^{\ddagger}$

(40) Casey, C. P.; Johnson, J. B. *Can. J. Chem.* **2005**, *83*, 1339.

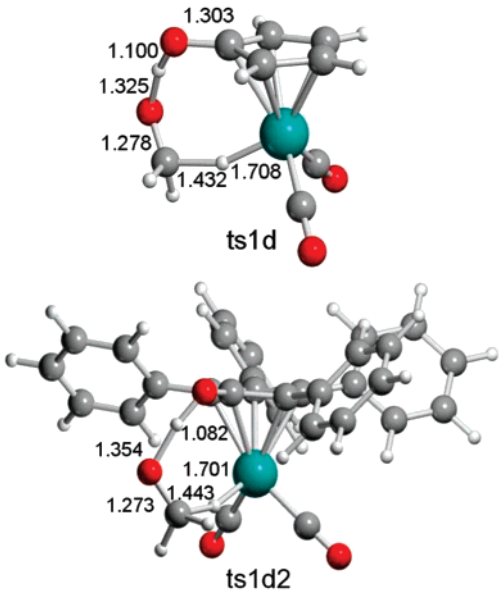

Figure 7. Transition state for the outer-sphere mechanism: model system (**ts1d**) and complete system (**ts1d2**). Distances in Å.

$= 12.0 \pm 1.5$ kcal/mol for the reduction of PhCHO in THF-d_8 in the presence of 0.1 mol/L of H_2O or D_2O[20] and $\Delta H^{\ddagger} = 11.2 \pm 0.9$ for the same process in dry THF-d_8.[40] Moreover, this mechanism is the most feasible one of all the analyzed pathways.

Model System versus Complete System. The concerted outer-sphere mechanism as well as the most favorable inner-sphere mechanism were analyzed taking for the calculations a complete Shvo catalyst, including four phenyl groups in the CpOH ring, [$Ph_4(\eta^5$-$C_4COH)$]. For the outer-sphere mechanism the analogous transition state **ts1d** was localized, with an energy of 1.9 kcal/mol in the gas phase. This value is quite similar to the one obtained for the model system (−1.5 kcal/mol), showing that the inclusion of the phenyl rings does not change significantly the results for the outer-sphere pathway. The energy barrier calculated is 8.8 kcal/mol, quite close to that of the model system, 9.1 kcal/mol.

For the most favorable inner-sphere mechanism (stepwise $\eta^5 \rightarrow \eta^2$ ring slippage) all the minima along the pathway were localized. The gas-phase energies for the model system intermediates **1b**, **2b**, **3b**, **4b**, and **5a** and final products (**b** + CH_3-OH) were −10.6, 18.0, 22.2, 17.8, −23.8, and −0.2 kcal/mol, respectively, related to separated reactants (see Figure 5). Exploring the potential energy surface for the complete system drove us to the localization of all the analogous intermediates found for the model system. Their relative energy values related to separated reactants are −6.9, 24.7, 27.6, 20.7, −22.4, and −0.9 kcal/mol for **1b′**, **2b′**, **3b′**, **4b′**, **5a′**, and final products (**b′** + CH_3OH), respectively. The highest and lowest energetic intermediates are the same for the model and the complete system, **3b**, **3b′**, and **4b**, **4b′**, respectively. The energy profile for the outer-sphere mechanism on the complete system is clearly energetically more favorable than that for the inner-sphere mechanism. The energy barrier for the outer-sphere mechanism is 8.8 kcal/mol, whereas the most stable intermediate for the inner-sphere mechanism (before formation of coordinated ethanol, **5a′**), **4b′**, has an energy of 20.7 kcal/mol. Therefore, calculations on the complete system give similar trends to those on the model system.

In the concerted transition state for the complete system,[41] **ts1d2** (see Figure 7), the O−H and Ru−H distances are 1.082 and 1.701 Å, respectively, whereas for the model catalyst these distances are slightly enlarged by 0.018 and 0.007 Å, for O−H and Ru−H distances, respectively. The length of the C−O bond of the formaldehyde in **ts1d2** is 1.273 Å, whereas that in **ts1d** (model system) was 1.278 Å. Hence, the inclusion of the phenyl substituents on the aromatic ring ligand has no significant effects on the transition state geometry.

The **1b2** and **2c2** geometries are the analogues of **1b** and **2c** for the model system. In **1b2** the distance of the hydrogen bond between the CpOH and the aldehyde oxygen is 1.807 Å. In **2c2**, there is also an agostic interaction through the newly formed C−H, revealed by the C−H distance of 1.146 Å. The recently formed OH bond has a distance of 0.981 Å. Like in **2c**, the hapticity of the ring is η^4, with the ring bonded to the metal through two double bonds formed in the ring after the hydrogen transfer. The four coordination carbons of the ring have distances with the ruthenium atom of 2.295, 2.252, 2.265, and 2.310 Å, respectively. The last carbon atom of the ring in **2c2** is out of the ring plane, as in **2c**, having a Ru−C distance of 2.468 Å, slightly shortened with respect to the model system, 2.507 Å. The distance of the C−O bond of the ring ligand in **2c2** is 1.381 Å. The OH group of the formed methanol is interacting through a hydrogen bond with the recently formed C═O group of the ring, characterized by a distance of 1.803 Å.

Calculation of Kinetic Isotope Effects. Casey and co-workers reported individual kinetic isotope effects in benzaldehyde hydrogenation using an analogue of the Shvo catalyst (where two Ph groups were substituted by two Tol groups) for the Ru−D and O−D bonds with values of 1.5 ± 0.2 and 2.2 ± 0.1, respectively, in THF in the presence of a small amount of water. On the basis of the agreement between the product of both individual isotope effects ($1.5 \times 2.2 = 3.3$) and the measured one for RuD−OD species (3.6 ± 0.3), they concluded that the hydrogenation takes place through a concerted proton and hydride transfer.[20] In a recent study, they showed that the addition of water to THF led to a decrease of the Ru−D kinetic isotope effect with a concomitant increase of the O−D kinetic isotope effect.[40] The combined isotope effect also was found to increase. In dry THF (at 22 °C) the individual isotope effects were 2.60 ± 0.09 for Ru−D and 1.30 ± 0.02 for O−D, whereas the combined isotope effect was 3.38 ± 0.19. Conversely, addition of water (0.120 mol/L) led to values of 1.32 ± 0.11 for Ru−D and 2.99 ± 0.35 for O−D, with a value of 4.25 ± 0.62 for the combined isotope effect. The authors also analyzed the KIEs in other solvents such as toluene and CH_2Cl_2; the reported kinetic isotope effects in these solvents are quite similar to the reported ones in dry THF (see Table 1).

In a parallel study by the group of Bäckvall on the dehydrogenation of 1-(4-fluorophenyl)ethanol by the Shvo catalyst, they reported KIEs of 1.87 ± 0.17 and 2.57 ± 0.26 for the rupture of O−H and C−H bonds of the alcohol, respectively, and the combined isotope effect of 4.61 ± 0.37, also supporting a concerted transfer.[22]

We have performed kinetic isotope effect calculations (KIEs) for both concerted mechanisms previously described. The free energy barriers used for KIE calculations are those between the initial reactants and the corresponding transition states. The obtained results are gathered in Table 1. For the outer-sphere

(41) The transition state **ts1d2** (for the complete system) was recalculated with Gaussian03. The geometries and energies obtained are very similar. The energy barriers found here were 8.3 and 8.0 kcal/mol in the gas phase and in solution, respectively.

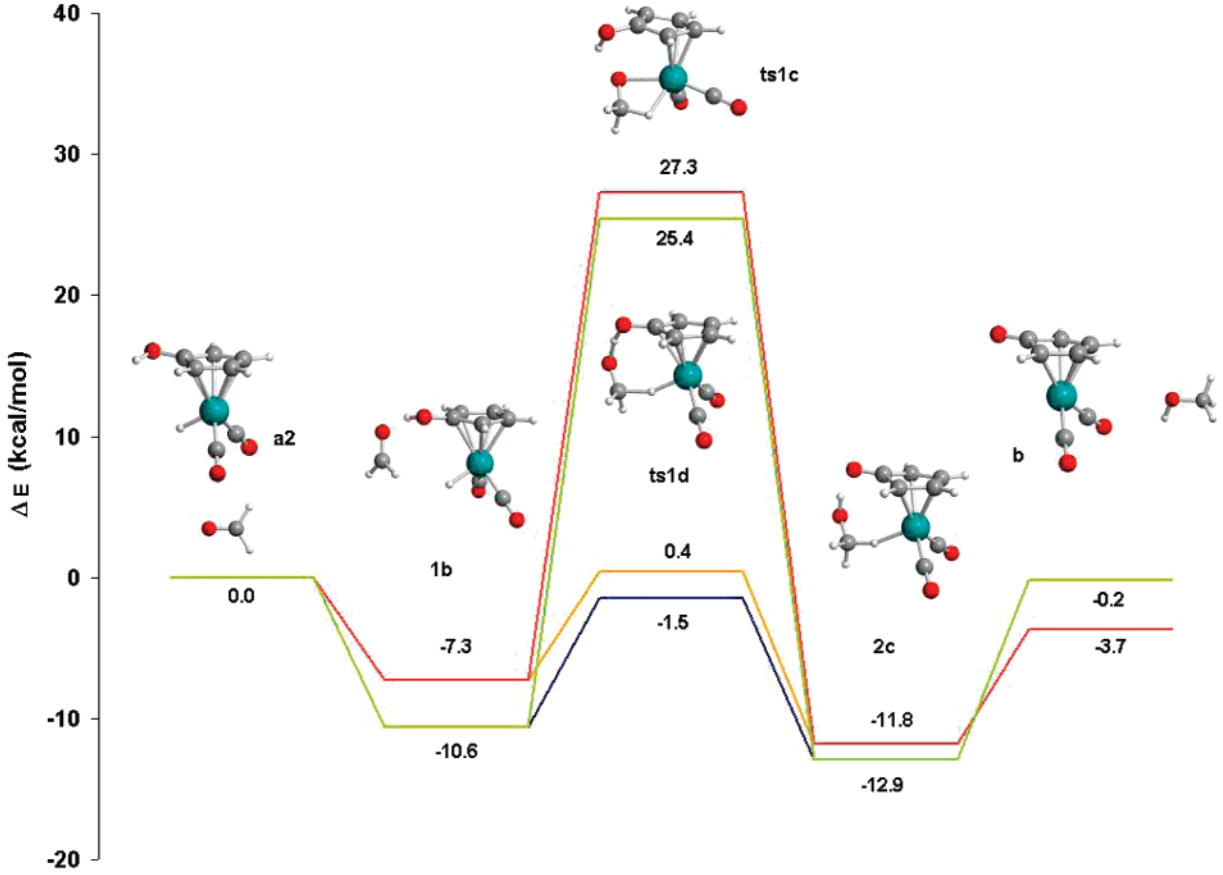

Figure 8. Energy profiles for both concerted pathways at the B3LYP level. Inner-sphere mechanism: green (gas phase) and red (solution), respectively. Outer-sphere mechanism: blue (gas phase) and orange (solution) respectively.

Table 1. Calculated Kinetic Isotope Effects for the Concerted Mechanisms Including the Experimental Values

mechanism	Ru−D bond	O−D bond	dideuterated species
concerted inner sphere	0.7	1.1	0.8
concerted outer sphere (model system)	1.3	3.1	3.8
concerted outer sphere (complete system)	1.3	2.8	3.5
THF (no water)[a]	2.60 ± 0.09	1.30 ± 0.02	3.38 ± 0.19
THF (0.120 mol/L water)[a]	1.32 ± 0.11	2.99 ± 0.35	4.25 ± 0.62
CH_2Cl_2[a]	2.51 ± 0.28	1.33 ± 0.13	3.36 ± 0.36
toluene[a]	2.65 ± 0.18	1.38 ± 0.08	3.63 ± 0.25
THF[b]	1.5 ± 0.2	2.2 ± 0.1	3.6 ± 0.3

[a] From ref 40. [b] From ref 20.

mechanism we calculated the KIEs for the model and the complete systems. The obtained values are similar in both cases, showing that the model system is good enough to study the system. Notice that all calculations were performed using formaldehyde as substrate, whereas the experimental values used benzaldehyde as substrate.

Our results, based on gas-phase calculations, are expected to be closer to the KIEs reported in toluene than the other solvents since it presents the lowest dielectric constant ($\epsilon = 2.4$). For the complete system in the outer-sphere mechanism, the value for the combined isotope effect is very close to the experimental one: 3.5 (calculated) versus 3.63 ± 0.25 (toluene). The individual isotope effects present a different trend. For Ru−D, we obtained a KIE value of 1.3 compared to the experimental value of 2.65 ± 0.18 (toluene). For the O−D bond the calculated value is 2.8 compared to the experimental value of 1.38 ± 0.08 (toluene). Surprisingly, theoretical values are closer to the individual kinetic isotope effects reported in THF with a small amount of water (see Table 1) than those in dry THF or toluene.

The value for the combined isotope effect for the concerted inner-sphere mechanism is quite different from the experimental value in toluene: 0.8 versus 3.63 ± 0.25. Concerning the individual isotope effects, the O−D bond agrees fairly well with the experimental value in toluene, whereas the Ru−D bond does not. The fact that the combined isotope effect is quite far from the experimental result does not support the concerted inner-sphere mechanism.

In conclusion, the calculated combined isotope effect for the outer-sphere mechanism is in better agreement with the experimentally reported values than that obtained for the concerted inner-sphere mechanism. Therefore, in accordance with the previous analysis of the energy reaction profiles, these results also suggest a concerted outer-sphere mechanism for the hydrogen-transfer process.

Conclusions

The hydrogen-transfer process to ketones catalyzed by the Shvo catalyst was extensively analyzed by means of DFT theoretical calculations. Several inner-sphere mechanisms (that imply the coordination of the substrate on the coordination sphere of the metal catalyst) and the outer-sphere mechanism (without substrate coordination) were considered. The energy profiles in the gas phase and including solvation effects for all the proposed mechanisms were calculated, and the KIEs for the most favorable concerted mechanisms were also evaluated.

According to our results, the most viable mechanism (that with the lowest energy barrier) is the outer-sphere mechanism where the hydrogen transfer takes place without coordination

of the substrate to the metal center; the proton and the hydride are transferred simultaneously to the C═O double bond. The energy barrier for the model system is 9.1 kcal/mol in the gas phase and 7.7 kcal/mol in solution (THF). For the complete system (where the entire Shvo catalyst was included in the calculations) these barriers adopted values of 8.3 and 8.0 kcal/mol in the gas phase and solution, respectively. The calculated KIEs for this mechanism are also in good agreement with the experimental reported ones.

Within the inner-sphere mechanisms, that involving the initial CO leaving is highly endothermic in the initial dissociative process. The energy barrier for this step is 51.2 kcal/mol in the gas phase and 45.7 kcal/mol in solution; the free energy barrier associated with this process in the gas phase is 38.7 kcal/mol. As expected, inclusion of entropic effects clearly diminishes the energy barrier for a dissociative process, although the barrier is still too high to be a feasible mechanism.

The inner-sphere mechanism involving the substrate coordination along with the ring slippage has an energy barrier in the gas phase of 34.3 kcal/mol, too high to be a feasible mechanism. A noticeable feature about this mechanism is that it involves a $\eta^5 \rightarrow \eta^2$ ring slippage instead of the initially proposed $\eta^5 \rightarrow \eta^3$ ring slippage. Our results are in agreement with previous studies on the ring slippage process on related transition metal complexes.

Concerning the concerted inner-sphere mechanism where the hydrogen transfer takes place simultaneously with the $\eta^5 \rightarrow \eta^3$ ring slippage, it has a barrier of 36.0 kcal/mol in the gas phase and 34.6 kcal/mol in solution. Despite being a concerted pathway, the energy barrier is too high compared with the outer-sphere mechanism. Moreover, the calculated combined kinetic isotope effect for this mechanism is clearly different from the experimentally reported value.

In summary, the feasibility of the outer-sphere mechanism (a concerted hydrogen transfer without carbonyl coordination) is supported by presenting the lowest energy barrier among all the studied processes and calculated KIEs closest to those obtained experimentally. These results are in agreement with other hydrogen-transfer processes based on metal−ligand bifunctional catalysts, even though this catalyst has the proton donor moiety quite far from the metal center. All reported studies to date suggest that metal−ligand bifunctional catalysts work through an outer-sphere mechanism. These conclusions may be applicable to the hydrogenation of other polar double bonds, and an analysis is in progress in our lab.

Acknowledgment. We are grateful to the Spanish MEC (Project CTQ2005-09000-C02-01, "Ramón y Cajal" contract to G.U. and FPU fellowships to A.C.-V), as well as to the Generalitat de Catalunya (2005/SGR/00896).

Supporting Information Available: Complete ref 30, absolute energies, and Cartesian coordinates. This material is available free of charge via the Internet at http://pubs.acs.org.

OM7004832